

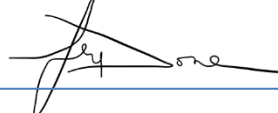
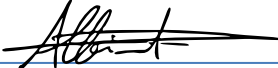




Technical Note on Quality Assessment for SkySat Video Data

Author(s): 

Sébastien Saunier
Sultan Kocaman
Task 1 Mission Expert

Approval: 
Fay Done
Task 1 Lead

Accepted: 
Clement Albinet
ESA Technical Officer

AMENDMENT RECORD SHEET

The Amendment Record Sheet below records the history and issue status of this document.

ISSUE	DATE	REASON
0.1	27 10 2021	Draft version for ESA review
1.0	23 03 2022	First issue

TABLE OF CONTENTS

1. INTRODUCTION.....	3
1.1 Reference Documents	3
1.2 Glossary	7
2. EDAP QUALITY ASSESSMENT	8
2.1 Maturity Matrix.....	8
2.2 Product Information	8
2.3 Product Generation	10
2.4 Ancillary Information.....	10
2.5 Uncertainty Characterisation	10
2.6 Validation.....	11
3. EDAP VALIDATION	14
3.1 Introduction.....	14
3.2 Input Data	14
3.3 Absolute Geolocation Accuracy	18
3.3.1 Method and tools	18
3.3.2 Results / Conclusion	19
3.4 Information Extraction Capability	21
3.4.1 Methods and tools	21
3.4.2 Results	22
APPENDIX A MISSION AND PRODUCT	25
A.1 Mission Description	25

1. INTRODUCTION

This Technical Note (TN) details the results regarding the assessment of SkySat (SKS) video products delivered by Planet.

The data quality of SkySat standard products has already been addressed and are reported into a dedicated TN [RD-6]. This latter document addresses most data accuracy parameters as part of geometric calibration, radiometric calibration and image quality topics. Finally, the overall quality of the mission is summarised into a dedicated quality maturity matrix, shown in Table 1-1. Therefore, for any issues regarding the quality of standard products, the reader is invited to refer to this TN document.

Table 1-1 SkySat Quality Maturity Matrix ([RD-6]) for Standard Product.

Product Information	Product Generation	Ancillary Information	Uncertainty Characterisation	Validation	Key
Product Details	Sensor Calibration & Characterisation Pre-Flight	Product Flags	Uncertainty Characterisation Method 🔒	Reference Data Representativeness	Not Assessed
Product Availability & Accessibility	Sensor Calibration & Characterisation Post-Launch 🔒	Ancillary Data	Uncertainty Sources Included 🔒	Reference Data Quality	Not Assessable
Product Format	Retrieval Algorithm Method		Uncertainty Values Provided 🔒	Validation Method	Basic
User Documentation	Retrieval Algorithm Tuning		Geolocation Uncertainty 🔒	Validation Results	Intermediate
Metrological Traceability Documentation	Additional Processing				Good
					Excellent

🔒 Information not public

The assessment of video data is an experimental exercise and the EDAP team is still developing assessment methodologies and protocols. An attempt has been made to remain consistent with the other EDAP TNs generated by EDAP. Also, the same set of maturity matrix parameters tailored to video data has been used and approach still relies on the two following activities:

- **Documentation Review:** the EDAP Optical team reviews materials provided by the data provider and / or operator (e.g. data and documentation), some of which may not be publicly available, or even the scientific community (e.g. published papers).
- **Data Quality Assessments:** the EDAP Optical team performs data quality assessments (i.e. validation assessments), independently of any validation assessments performed by the data provider and / or operator. The results are detailed in Section 3 (covering the last column, 'Validation', of the maturity matrix).

1.1 Reference Documents

The following is a list of reference documents with a direct bearing on the content of this proposal. Where referenced in the text, these are identified as [RD-n], where 'n' is the number in the list below:

RD-1. EDAP.REP.001 Generic EDAP Best Practice Guidelines, 1.1 23 May 2019

- RD-2. EDAP.REP.002 Optical Mission Quality Assessment Guidelines, 1.0, 16 October 2019.
- RD-3. Planet Imagery Product Specifications, February 2021, https://assets.planet.com/docs/Planet_Combined_Imagery_Product_Specs_letter_scren_image_processing_chain.jpg.pdfs
- RD-4. Planet BASIC L1A All-Frames USER GUIDE, February 2021. https://assets.planet.com/docs/Planet_Basic_L1A_All-Frames_User_Guide.pdf
- RD-5. Planet L1 Data Quality Report Q3 2020 – Status of calibration and Data Quality for the SKYSAT Constellation
- RD-6. EDAP Technical Note on Quality Assessment for SkySat. EDAP.REP.015. 0 Issue 1.0. 06.09.2021 https://earth.esa.int/eogateway/documents/20142/37627/EDAP.REP.015+TN+on+Quality+Assessment+for+SkySat_v1.0.pdf/59a2a91d-eeed-20f1-4a13-e670dad8eed3
- RD-7. Du, B., Sun, Y., Cai, S., Wu, C., & Du, Q. (2017). Object tracking in satellite videos by fusing the kernel correlation filter and the three-frame-difference algorithm. *IEEE Geoscience and Remote Sensing Letters*, 15(2), 168-172.
- RD-8. Du, B., Cai, S., & Wu, C. (2019). Object tracking in satellite videos based on a multiframe optical flow tracker. *IEEE Journal of Selected Topics in Applied Earth Observations and Remote Sensing*, 12(8), 3043-3055.
- RD-9. Guo, Y., Yang, D., & Chen, Z. (2019). Object tracking on satellite videos: A correlation filter-based tracking method with trajectory correction by Kalman filter. *IEEE Journal of Selected Topics in Applied Earth Observations and Remote Sensing*, 12(9), 3538-3551.
- RD-10. Xuan, S., Li, S., Han, M., Wan, X., & Xia, G. S. (2019). Object tracking in satellite videos by improved correlation filters with motion estimations. *IEEE Transactions on Geoscience and Remote Sensing*, 58(2), 1074-1086.
- RD-11. Hu, Z., Yang, D., Zhang, K., & Chen, Z. (2020). Object tracking in satellite videos based on convolutional regression network with appearance and motion features. *IEEE Journal of Selected Topics in Applied Earth Observations and Remote Sensing*, 13, 783-793.
- RD-12. Xuan, S., Li, S., Zhao, Z., Zhou, Z., Zhang, W., Tan, H., ... & Gu, Y. (2021). Rotation adaptive correlation filter for moving object tracking in satellite videos. *Neurocomputing*, 438, 94-106.
- RD-13. d'Angelo, P., Kusch, G., & Reinartz, P. (2014). Evaluation of skybox video and still image products. *The International Archives of the Photogrammetry, Remote Sensing and Spatial Information Sciences*, Volume XL-1, 2014, ISPRS Technical Commission I Symposium, 17 – 20 November 2014, Denver, Colorado, USA. <https://elib.dlr.de/93532/1/isprsarchives-XL-1-95-2014.pdf>
- RD-14. Anger, J., Ehret, T., & Facciolo, G. (2021). Parallax estimation for push-frame satellite imagery: application to super-resolution and 3D surface modeling from Skysat products. *arXiv preprint arXiv:2102.02301*.
- RD-15. Bhushan, S., Shean, D., Alexandrov, O., & Henderson, S. (2021). Automated digital elevation model (DEM) generation from very-high-resolution Planet SkySat triplet stereo and video imagery. *ISPRS Journal of Photogrammetry and Remote Sensing*, 173, 151-165.

- RD-16. Aati S, Avouac J-P. Optimization of Optical Image Geometric Modeling, Application to Topography Extraction and Topographic Change Measurements Using PlanetScope and SkySat Imagery. *Remote Sensing*. 2020; 12(20):3418. <https://doi.org/10.3390/rs12203418>
- RD-17. Wan, X., Liu, J., Yan, H., Morgan, G.L. and Sun, T., 2016, July. 3D super resolution scene depth reconstruction based on SkySat video image sequences. In 2016 IEEE International Geoscience and Remote Sensing Symposium (IGARSS) (pp. 6653-6656). IEEE.
- RD-18. Biron Smiley, "Long Term Geometric Stability of the SkySat Constellation" Processing of JACIE Conference, September, 19 2018
- RD-19. Planet L1 Data Quality Report Q3 2020 – Status of calibration and Data Quality for the SKS Constellation
- RD-20. d'Angelo, P., Mátyus, G., & Reinartz, P. (2016). Skybox image and video product evaluation. *International Journal of Image and Data Fusion*, 7(1), 3-18.
- RD-21. https://docs.opencv.org/4.5.2/d4/dc6/tutorial_py_template_matching.html
- RD-22. OpenCV cv::Tracker Class Reference
https://docs.opencv.org/3.4.15/d0/d0a/classcv_1_1Tracker.html
- RD-23. Kopsiaftis, G. and Karantzalos, K., 2015, July. Vehicle detection and traffic density monitoring from very high resolution satellite video data. In *2015 IEEE International Geoscience and Remote Sensing Symposium (IGARSS)* (pp. 1881-1884). IEEE.
- RD-24. Pflugfelder, R., Weissenfeld, A. and Wagner, J., 2020. On learning vehicle detection in satellite video. *arXiv preprint arXiv:2001.10900*.
- RD-25. Shu, M., Zhong, Y. and Lv, P., 2021. Small moving vehicle detection via local enhancement fusion for satellite video. *International Journal of Remote Sensing*, 42(19), pp.7189-7214.
- RD-26. Zhang, J., Jia, X. and Hu, J., 2019. Local region proposing for frame-based vehicle detection in satellite videos. *Remote Sensing*, 11(20), p.2372.
- RD-27. Feng, J., Zeng, D., Jia, X., Zhang, X., Li, J., Liang, Y. and Jiao, L., 2021. Cross-frame keypoint-based and spatial motion information-guided networks for moving vehicle detection and tracking in satellite videos. *ISPRS Journal of Photogrammetry and Remote Sensing*, 177, pp.116-130.
- RD-28. Zhang, J., Jia, X., Hu, J. and Tan, K., 2021. Moving Vehicle Detection for Remote Sensing Video Surveillance with Nonstationary Satellite Platform. *IEEE Transactions on Pattern Analysis & Machine Intelligence*, (01), pp.1-1.
- RD-29. Bhushan, S., Shean, D.E., Jordahl, K.A., Martos, A., Alexandrov, O., Henderson, S.T. and Kington, J.D., 2020, December. Automated DEM generation and scientific applications of Planet SkySat triplet stereo and video imagery. In *AGU Fall Meeting Abstracts* (Vol. 2020, pp. IN023-0006).
- RD-30. Shi, F., Qiu, F., Li, X., Tang, Y., Zhong, R. and Yang, C., 2020. A method to detect and track moving airplanes from a satellite video. *Remote Sensing*, 12(15), p.2390.
- RD-31. Wang, X., Li, F., Xin, L., Ma, J., Yang, X. and Chang, X., 2019, July. Moving targets detection for satellite-based surveillance video. In *IGARSS 2019-2019 IEEE International Geoscience and Remote Sensing Symposium* (pp. 5492-5495). IEEE.

- RD-32. Ahmadi, S.A., Ghorbanian, A. and Mohammadzadeh, A., 2019. Moving vehicle detection, tracking and traffic parameter estimation from a satellite video: a perspective on a smarter city. *International journal of remote sensing*, 40(22), pp.8379-8394.
- RD-33. Meng, Y., Wang, X. and Yuan, S., 2021, September. Vehicle detection base on Road Segmentation for surveillance satellites video. In *Journal of Physics: Conference Series* (Vol. 2010, No. 1, p. 012169). IOP Publishing.
- RD-34. Legleiter, C.J. and Kinzel III, P.J., 2021. Surface flow velocities from space: Particle image velocimetry of satellite video of a large, sediment-laden river. *Frontiers in Water*, 3, p.53.
- RD-35. Yang, T., Wang, X., Yao, B., Li, J., Zhang, Y., He, Z. and Duan, W., 2016. Small moving vehicle detection in a satellite video of an urban area. *Sensors*, 16(9), p.1528.
- RD-36. Chen, R., Li, X. and Li, S., 2020. A Lightweight CNN Model for Refining Moving Vehicle Detection From Satellite Videos. *IEEE Access*, 8, pp.221897-221917.
- RD-37. Li, H. and Man, Y., 2016, July. Moving ship detection based on visual saliency for video satellite. In *2016 IEEE International Geoscience and Remote Sensing Symposium (IGARSS)* (pp. 1248-1250). IEEE.
- RD-38. DING, Y. and WANG, Y., 2021. A Long-term Tracking Algorithm of Space-based Targets Based on Multi-feature Integration. *Spacecraft Recovery & Remote Sensing*, 42(4), pp.46-56.
- RD-39. Zhang, X., Xiao, L., Hu, M. and Liu, J., 2019, October. Scene matching method of video satellite remote sensing image based on deep convolutional neural network. In *2019 IEEE 1st international conference on civil aviation safety and information technology (ICCASIT)* (pp. 211-215). IEEE.
- RD-40. Zhang, J., Jia, X. and Hu, J., 2018, July. An Effective Zoom-In Approach for Detecting DIM and Small Target Proposals in Satellite Imagery. In *IGARSS 2018-2018 IEEE International Geoscience and Remote Sensing Symposium* (pp. 7074-7077). IEEE.
- RD-41. Xia, W., Guo, Z., Xin, S., Beibei, L.I. and Yonghua, J.I.A.N.G., 2016. Satellite video stabilization with geometric distortion. *Acta Geodaetica et Cartographica Sinica*, 45(2), p.194.
- RD-42. Zhu, K., Zhang, X., Chen, G., Tan, X., Liao, P., Wu, H., Cui, X., Zuo, Y. and Lv, Z., 2021. Single Object Tracking in Satellite Videos: Deep Siamese Network Incorporating an Interframe Difference Centroid Inertia Motion Model. *Remote Sensing*, 13(7), p.1298.
- RD-43. d'Angelo, P., & Reinartz, P. (2021). Digital Elevation Models from Stereo, Video and Multi-View Imagery Captured by Small Satellites. *International Archives of the Photogrammetry, Remote Sensing and Spatial Information Sciences*, 43, B2-2021.
- RD-44. Jiaqi, W. U., Guo, Z., Taoyang, W., & Yonghua, J. I. A. N. G. (2017). Satellite video point-target tracking in combination with motion smoothness constraint and grayscale feature. *Acta Geodaetica et Cartographica Sinica*, 46(9), 1135.

1.2 Glossary

The following acronyms and abbreviations have been used in this report.

ATBD	Algorithm Theoretical Basis Document
AC	ACros track
AL	ALong track
CCD	Charge-Coupled Device
CEOS	Committee on Earth Observation Satellites
EDAP	EarthNet Data Assessment Pilot
ESF	Edge Spread Function
FWHM	Full Width at Half Maximum
GCP	Ground Control Points
GeoJSON	Geographic JSON
HR	High Resolution
IFOV	Instantaneous Field of View
JACIE	Joint Agency Commercial Imagery Evaluation
LSF	Line Spread Function
MTF	Modular Transfer Function
NPL	National Physical Laboratory
PDI	Product Data Item
RMSE	Root Mean Square Error
SNR	Signal to Noise Ratio
SKS	SkySat
TN	Technical Note
TOA	Top-Of-Atmosphere
UDM2	Usable Data Mask
VHR	Very High Resolution

2. EDAP QUALITY ASSESSMENT

An attempt has been made to remain consistent with previous studies. Also, the same set of maturity matrix parameters tailored to video data has been used and the results are reported herein.


2.1 Maturity Matrix

A maturity matrix is in general associated to a mission and not a product type (e.g. video). As mentioned before, the information collected on the SkySat mission is captured into the main EDAP TN [RD-6]. It is a reference regarding all items referring to the raster product. On the other hand, concerning video data, the video data quality maturity matrix as a mean to summarise the quality at a higher-level is shown in Table 2-1. It is important to note that this approach is experimental because it is referring exclusively to the video data product only.

Table 2-1 SKS Video Data Quality Maturity (experimental)

Parameters	EDAP Results (key)
Product Information	Intermediate
Product Generation	Not Assessable
Ancillary Information	Good
Uncertainty Characterisation	Basic
Validation	Basic

Key
Not Assessed
Not Assessable
Basic
Intermediate
Good
Excellent

 Information not public

2.2 Product Information

This section covers top-level product description information, product format, and the supporting documentation.

The table below details general product information for SKS video data. For some parameters, values are directly accessible from the product format (written within the GeoJSON file), but the rest is available in documentation opened to the user.

Product Details	
Product Name	<i>Video Scene Product Basic Scene Product (Level 1A)</i>
Sensor Name	<i>SkySat</i>
Sensor Type	<i>CMOS Frame Camera (Multi-Spectral and Panchromatic) Video is produced with Panchromatic Image only</i>
Mission Type	<i>Satellite Constellation</i>

Mission Orbit	<i>Low Earth Sun Synchronous Orbit</i>
Product Version Number	<i>The product version number of the product is not tagged in the product format.</i>
Processor Name / Version	<i>The processor name or version that generated the product is not tagged in the product format.</i>
Product ID	<i><AcquisitionDate>_<AcquisitionTime>_<SatelliteID><CameraID>_<FrameId> Example: 20200718_082806_ssc4d1_0008</i>
Processing level of product	<i>Level 1A (As discussed below, the video file is delivered together with L1A products used to product the video).</i>
Measured Quantity Name	<i>Digital number to Radiance (SI) and Top of Atmosphere Reflectance (SI)</i>
Measured Quantity Units	<i>Not available in the metadata (DN / W sr⁻¹ m⁻² μm⁻¹)</i>
Stated Measurement Quality	<i>Unavailable</i>
Spatial Resolution	<i>The ground sampling distance (GSD) depends on the satellite altitude. Whatever the sensor band (Multispectral, Panchromatic), the GSD is within 0.6 m and 0.95 m. The GSD of video data image (Panchromatic) is 0.81 m. The Level 1A image (one video frame) is not projected with respect to a cartographic grid.</i>
Spatial Coverage	<i>The spatial coverage is given in the GeoJSON file with the geographical coordinates of the product footprint (corners). (For information, the image size of one basic scene (one camera) is about 2560 pixels x 1080 pixels (image width / image height), applicable for multispectral and panchromatic data.)</i>
Temporal Resolution	<i>The temporal resolution is not indicated as metadata information. The temporal resolution should not exceed one day accounting for the overall information.</i>
Temporal Coverage	<i>The temporal coverage understood as the scene time duration is not indicated in the product metadata.</i>
Video Duration	<i>The video duration is detailed as part of video product metadata (start / end time of the capture)</i>

The video product includes a video file together with all video frames and their corresponding ancillary information. Planet adopted the following breakdown for video product packaging ([RD-3]):

- The video file itself, produced in mpeg-4 (MP4) format,
- The video frame folder, including all images captured within the video observation period, the images are processed into the Planet Basic Level-1A product format specification, together with rational polynomial coefficients (RPC) file, pinhole camera model and frame index file (CSV), information given for every frame,
- The video metadata file (JSON).

Full motion videos are collected between 30 and 120 seconds by a single camera from any of the SkySat satellites and each corresponds to a specific observation mode. Videos are collected using the panchromatic half of the camera, hence all videos are built up based on panchromatic images.

The good amount of information available in the video product format. Additional information exists in the user guide [RD-3, RD-4]. This item is evaluated as “Intermediate”.

2.3 Product Generation

The video data are produced from the Level 1A frames and provided in mpeg-4 (**MP4**) format. The co-registration step for the video production is not provided by the vendor. According to [RD-13], the video product can be delivered in different formats, a stabilised Full HD video in MP4 format, where all video frames have been co-registered, and an unstabilised video without co-registration.

The product generation section covers the processing steps undertaken to produce the video data, including the calibration algorithm, retrieval algorithm and additional processing. The video product generation considers as input a set of Basic Level 1A products observed within the period of the video data recording, satellite command set in full motion video mode.

The Basic Level 1 products are discussed in the [SkySat TN](#) [RD-6].

It is important to note the Basic Level 1A product are without any geometric correction, in particular geo referencing by using Ground Control Points.

There is no information from the data provider regarding product generation of video data, this item is evaluated as “Not Assessable”.

2.4 Ancillary Information

The important video data specs and ancillary information can be listed as following:

- Image format
- Video format
- Time tags
- The radiometric, spectral and spatial resolutions
- Radiometric and geometric pre-processing methods and uncertainty information
- Reference coordinate system
- Auxiliary data for image orientation (e.g., RPCs, pinhole model, etc.)
- Satellite platform and sensor position and orientation information
- Video processing method
- Video frame rate

As previously mentioned, together with the documentation, it is possible for expert user to produce video data with his own parameter tuning. The EDAP grade for this item is ‘Good’.

2.5 Uncertainty Characterisation

[HOW IDEALLY TO REPORT ON VIDEO DATA QUALITY]

This section of the mission quality assessment evaluates the methodology used to estimate uncertainty values for a given mission, the extent of the mission’s assessment and how the values are provided.

As shown in SKS TN [RD-6], the Planet team performs regular uncertainty characterisation activities as illustrated in the quarterly data quality report [RD-5].

Considering the application fields of the video data (e.g., object detection and tracking, digital elevation model generation, etc.) and the specifications of the Level 1A images which are input, it is interesting to focus on the following parameters:

- Absolute geolocation (direct georeferencing) accuracy
- DEM production capability and quality (optimal baselines, height accuracy, completeness, consistency, etc.)
- Radiometric quality and coherence between the frames for video quality, optimal detection and tracking
- Geometric quality and coherence between the frames for video quality, motion detection and tracking computation

The table below details the geolocation uncertainty results given by the data provider.

Geolocation Uncertainty	
Summary	<p>The product accuracy results (Level 1A) reported by the quality control team [RD-5] and considered as EDAP input specifications [RD-3] can be summarised as follow:</p> <ul style="list-style-type: none"> • <i>The absolute geolocation accuracy is 70.3 m for basic scene products defined as average distance. This average accuracy is computed based on 40696 products,</i>
Reference	[RD-5]

The specification for the absolute geolocation accuracy of Level 1A products is < 50 m as described in RMSE [RD-3].

It is worth noting, that the actual accuracy values were not assessed for the Level 1A products by the quality control team of Planet [RD-5]. Therefore, the specification given in the [RD-3] is considered here for the validation. The specification does not include the expected elevation accuracy. Therefore, the DEM generation quality efforts cannot be evaluated with respect to the specification.

The notion of uncertainty attached to video product is not defined in the community. Taking into account before mentioned parameters, the EDAP grade is 'basic'.

2.6 Validation

The below validation items are related to activities conducted by the EDAP Team (not Planet).

As mention before, the topic of video data validation methodology in EDAP is relatively new and not established yet. The EDAP team validated the video data by addressing these two data quality items:

- The absolute geolocation accuracy of the video frames;
- The information extraction capability and the issues with the motion tracking capability including object detection.

The absolute geolocation accuracy validation relies on the external reference data.

Reference measurements are assessed to be somewhat representative of the satellite measurements, covering a limited range of satellite measurements. For this reason, the EDAP grade of **Reference Data Representativeness** is 'Basic'.

The reference data used by EDAP comes with a single uncertainty for the entire data set. For this reason, the EDAP grade of **Reference Data Quality** is 'Intermediate'.

Reference Data Quality	
Summary	<p>Regarding the absolute geolocation, the method used as reference a GCP set derived from a GPS test field survey. The uncertainty of the field measurement is within 2-3 cm. The multi-temporal accuracy is also assessed by using the same GCP set.</p> <p>The stereoscopic capability assessment was performed by comparison of Skysat-generated DSM with UAV-DSM. The UAV-DSM has a global uncertainty value of approximately 5 cm. It is worth noting that for this analysis UAV DSM data is used as supporting data. No stereoscopic capability assessment has been performed.</p>
Reference	Approximate center coordinate of the Ankara test site: Lat: 39°56' Lon: 33° 0' E defined in EPSG 4326

The EDAP methodology assess satellite measurements providing a simple uncertainty estimated (e.g. from statistical point of view). For this reason, the EDAP grade of **Validation Method** is 'Intermediate'.

Validation Method	
Summary	The absolute geolocation accuracy
Reference	See section 2.

Validation Method	
Summary	The information extraction capability of the video sequence was assessed based on the object detection capability and the motion tracking capability. Here, the size of the objects detected and various issues observed in the results are used for preliminary assessment.
Reference	See section 3.

For any analysis, the compliance between the validation results and data provider specification is shown in Table 2-2. Validation results demonstrates an overall agreement between satellite and reference measurements and agreement is in most cases within uncertainties claimed by the data provider.

All EDAP validation analyses are detailed in Section 3. Furthermore, the EDAP analysis have been performed independently from the satellite mission owner. As result, the EDAP grade if **Validation Results** is "Good".

Table 2-2 - EDAP Validation Analysis Results.

EDAP Validation Analysis	Compliance (Y / N)
Product Documentation	Y
Product Format	Y
Image Quality / Visual Inspection	Y

Geometric Quality / Absolute Geolocation	Y
Geometric Quality / Temporal Registration	NA*
Geometric Quality / Stereoscopic Capability	NA*
Video Stability / Object tracking capability	Y

* As there is no input specification regarding stereoscopic capability (elevation accuracy), the compliance item has been set to Not Available (NA).

When the literature is analysed, the following assessments were performed with the SkySat video products:

- Stereo capability and DEM elevation accuracy (e.g. [RD-15, RD-20, RD-17, RD-14, RD-43, RD-29, RD-16]);
- Direct georeferencing and RPC quality (e.g. [RD-15, RD-20, RD-43, RD-29, RD-26, RD-16, RD-34]);
- Radiometric quality (coherence between frames, video stabilisation, image noise, radiometric bit depth, histogram analysis) [RD-20, RD-34, RD-41];
- Motion analysis [RD-38, RD-42] and vehicle speed measurement [RD-20];
- Vehicle detection (cars, buses, large trucks) [RD-20, RD-22, RD-11, RD-24, RD-27, RD-25, RD-44, RD-31, RD-32, RD-28, RD-33, RD-35, RD-36, RD-38, RD-40, RD-42];
- Airplane detection [RD-30] and tracking (without georeferencing) [RD-30];
- Ship detection [RD-37];
- Traffic density monitoring [RD-22, RD-32];
- Automated image-vector database matching (i.e., image to road database matching) [RD-20];
- River velocity estimation [RD-34];
- Image Frame Rate [RD-34];
- Scene matching capability [RD-39].

3. EDAP VALIDATION

3.1 Introduction

Considering the innovative and often challenging technology associated with Very High Resolution (**VHR**) and High Resolution (**HR**) data, this TN reports the results of the performed quality assessments with respect to the following validation aspects:

- Absolute Geolocation Accuracy of input data
- Stability of Video Sequence including the object detection capability and the motion tracking capability

The stability of a video sequence can be appreciated from different point of views, the radiometric stability (exposure adaptation) and the geometric stability.

The image quality of one single image frame has been addressed in the previous SKS TN. The previous SKS TN focused on user products (Level 1C) for which radiometric equalisation, geometric resampling and post processing makes image quality better. In case of video data, Level 1A images are used. Also, video data processing includes cosmetic processing dedicated to radiometric equalisation between successive frames. Indeed, it is expected that the luminance does not vary within the movie (histogram adjustment).

As mentioned before, the Level 1A images are not projected. The relationship between image space and object space is not straightforward in the video, and it is technically very difficult to ensure. Although, from user point of view, retrieving geolocation information associated with motion tracking results implies to use RPC files attached to each image frame. For this reason, the assessment of absolute location of input data is fundamental.

An important parameter is also the geographical footprint of the video frames that should remain the same during the video period. The satellite is moving, attitude and instrument control are always calibrated to ensure the best pointing stability. There are motions (platform, instrument) that are statistically uncorrelated, making quantitative analysis complex; it is for instance expected that a fixed target, remains at the same image location in the different frames.

To summarise, quality of motion tracking, object extraction strongly depends on the radiometry, geometry and more generally on satellite / instrument technical specifications.

3.2 Input Data

The video dataset evaluated within EDAP includes two mpeg-4 files acquired over Ankara Test Site (Figures 1-3). The site was already used for SkySat evaluations and reported in [RD-6]. The specifications of the video files are presented in Table 3-1.

Here, it must be noted that the Geotiff geographical coordinates of the frames were used in the desktop GIS software for the overlay, as shown in figure below. The actual absolute geolocation assessments were performed using the associated RPC file of each frame, applying a specific methodology.

The evaluation site was selected based on the land cover characteristics (e.g., availability of large roads with junctions) mainly for the purpose of motion tracking capability assessment.

For both analyses (geolocation, video data stability), the following dataset has been used.

Table 3-1 SkySat video product, input EDAP dataset (L1A scenes and video)

ID	Product Name	Duration & GSD	Acquisition Date Satellite/Location
PDT1	1307610184.98412180_sc00003 s3_20210613T090247Z	30 sec & 1.02 m GSD	13 June 2021, SKS3, Ankara, Turkey; Extent: UL Lon/Lat: 32.98694°, 39.94698°; LR Lon/Lat: 33.02023°, 39.96184°
PDT2	1308482688.04125881_sc0108 s108_20210623T112430Z	30 sec & 0.91 m GSD	23 June 2021, SKS108 (TBC), Ankara, Turkey; Extent: UL Lon/Lat: 32.98400°, 39.9145°3; LR Lon/Lat: 33.01071°, 39.92612°

Note that metadata file of the product has been part of the delivery performed by Planet, also product names are exotic with some doubts on satellite involved.

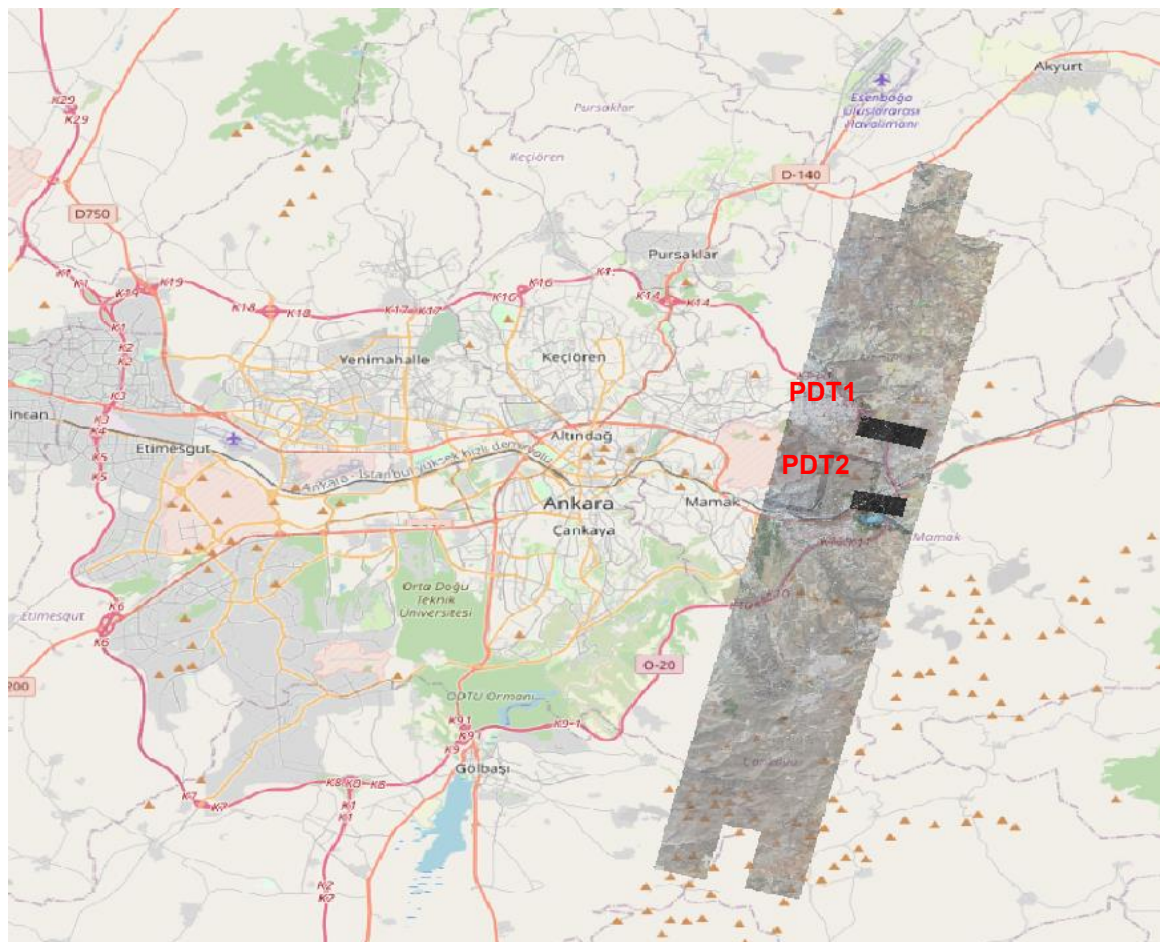


Figure 3-1. Location of Ankara test site shown on OpenStreetMap web map, SkySat ortho acquired on 18 July 2020 and used in SkySat TN [RD-6] and the coverage of the video products used for validation in this report.



Figure 3-2 Zoomed view of PDT1 and PDT2 used for validation in this report.



Figure 3-3. SkySat video data displayed with end user movie player.

The properties of the two movie files are listed in tables below. The bit rate of the two is different, these parameters are not explained by the data provider.

Informations		Informations	
Propriétés		Propriétés	
ExifTool		ExifTool	
Fichier		Fichier	
Nom de fichier	Project_67475_Turkey_Video_1.mp4	Nom de fichier	Project_67475_Turkey_Video_2.mp4
Répertoire	F:\2020_SKYSAT_50\In_data\VIDEO_DATA	Répertoire	F:\2020_SKYSAT_50\In_data\VIDEO_DATA
Description	MP4 Video File (VLC)	Description	MP4 Video File (VLC)
Taille de fichier	19.89 Mio (20 851 716)	Taille de fichier	9.32 Mio (9 777 745)
Date/Heure de création	28/06/2021 - 15:33:26	Date/Heure de création	28/06/2021 - 11:45:00
Date/Heure de modification	28/06/2021 - 15:33:36	Date/Heure de modification	28/06/2021 - 11:45:00
Date/heure d'accès	22/10/2021 - 18:54:01	Date/heure d'accès	22/10/2021 - 18:54:52
Note	Pas de note	Note	Pas de note
Libellé de couleur	Non coloré	Libellé de couleur	Non coloré
Image		Image	
Format	8577467557567467567567568567567567567567	Format	7667456557567567567
Largeur	909456693	Largeur	926233909
Hauteur	892679734	Hauteur	926365495
Nb bits	195310991	Dimension	4.7e+02 Mpixels
Modèle couleur	RGB	Nb bits	192324396
PPI	13367 x 13878	Modèle couleur	RGB
Taille d'impression	-692.92x-643.18 cm, 68037.46x64323.37 pouces	PPI	13622 x 14135
Compression	Uncompressed	Taille d'impression	-704.58x-655.36 cm, 67995.44x65537.00 pouces
Nb images/pages	892679991	Compression	Uncompressed
Origine	Haut gauche	Nb images/pages	909391926
Vidéo		Vidéo	
Format	AVC	Format	AVC
Largeur	2560	Largeur	2560
Hauteur	1080	Hauteur	1080
Durée	30 s 5 ms	Durée	30 s 4 ms
Bit rate	5 557 kb/s	Bit rate	2 604 kb/s
Aspect ratio	2.40:1	Aspect ratio	2.40:1
Frame rate mode	CFR	Frame rate mode	CFR
Frame rate	30.000	Frame rate	30.000
Audio		Audio	

Figure 3-4. SkySat video data specs shown in Windows File System (XnView).

An overview of the “s3_20210613T090247Z” Level 1A frame products (first, middle and last frames of the video) overlaid on the Skysat ortho collect product is shown in Figure 3.1. The Figure shows the georeferencing quality of Geotiff data. The quality of Geotiff files is poorer than the RPC files due to the inclusion of only 2D position information in the former one. Consequently, large geolocation shift is observed – the purpose being only to quickly show images. Natively, accurate co-registration of Level 1A is not reached. The use of RPC file is required.



Figure 3-5. An overview of the s3_20210613T090247Z all frames product (first, middle and last frame) overlaid on the Skysat ortho collect product.

3.3 Absolute Geolocation Accuracy

The geolocation accuracy of some selected input image frame in the video has been assessed from relative and absolute accuracy point of view.

3.3.1 Method and tools

The methodology for the absolute geolocation accuracy assessment is based on external reference, i.e. GCPs surveyed by using Global Navigation Satellite System (**GNSS**) instruments, over Ankara (Turkey) test site.

Two GCPs were measured on a total of five selected frames obtained from the two videos. The evaluations were carried out by using the backprojection of GCP ground coordinates to the panchromatic image coordinates using RPC files provided by the vendor; and comparative evaluation of the backprojected coordinates with the measured image coordinate values in x (row) and y (column) directions by using statistical metrics (i.e. mean, absolute mean, median, standard deviation and RMSE).

The basic depiction of the RPC backprojection method can be found in [RD-6]. The input of the coordinate transformation function for every point is Latitude, Longitude and Height values and the given RPCs are used in the rational polynomial functions with the inputs. The output of the backprojection function is line and sample (or row and column)

coordinates in image space. The measured and the output coordinates of the five points were compared for the absolute geolocation accuracy assessment.

Basic Scene products (2D assessment): Backprojection of GCP ground coordinates to the panchromatic image coordinates using RPC files provided by the vendor; and comparative evaluation of the backprojected coordinates with the measured image coordinate values in x (row) and y (column) directions by using statistical metrics (i.e. mean, absolute mean, median, standard deviation and RMSE). See Figure 3-6 for the basic depiction of the RPC backprojection method. The input of the coordinate transformation function for every point is Latitude, Longitude and Height values and the given RPCs are used in the rational polynomial functions with the inputs. The output of the backprojection function is line and sample (or row and column) coordinates in image space.

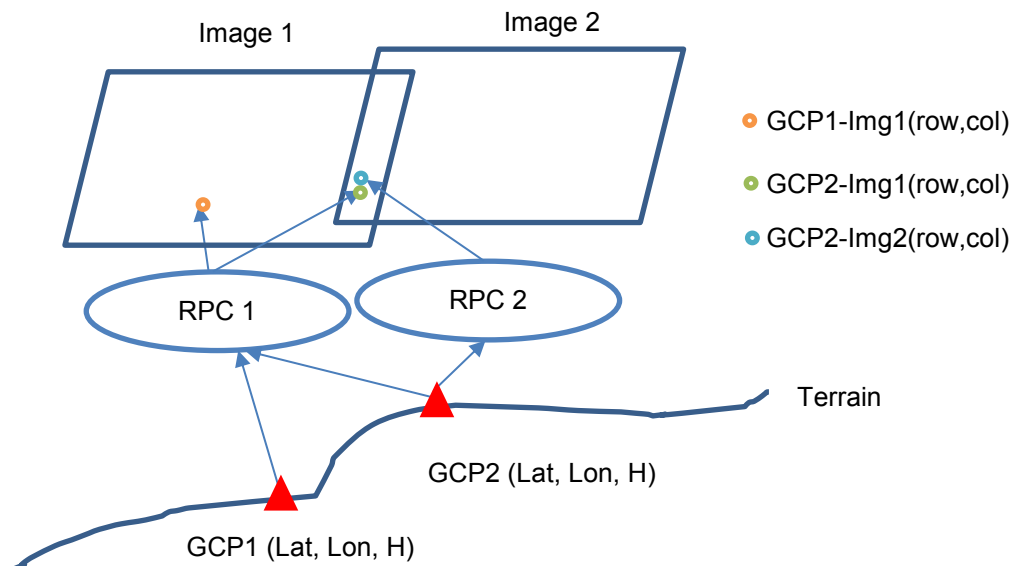


Figure 3-6. RPC backprojection method [RD-6].

3.3.2 Results / Conclusion

The absolute geolocation assessment results obtained from the five measurements are presented in Tables 3.2 and 3.3. The first and the last frames of s3_20210613T090247Z product were evaluated using the GCP numbered P20. The first, the middle and the last frames of s108_20210623T112430Z all frames product were assessed using P03. The P20 was not visible in the middle frame of the 20210613T090247Z product. The x and y axes are defined in image space, but roughly represent the Easting and Northing directions, respectively. The discrepancies (dx, dy) between the measured and the backprojected image space coordinates are given in Table 3-2. The results obtained from the five measurements are statistically summarized in Table 3-3.

The detailed results in Table 3.2 show that the accuracy variations between the different frames can be over 25 pixels (relative accuracy). These values represent the geometric quality of individual RPC files, and not the co-registration quality of the video frames.

Table 3-2 SkySat video data used for the absolute geolocation assessment

GCP ID	Video Product ID	Frame Number	dx (pixel)	dy (pixel)	dx (m)	dy (m)
P20	PDT1	0 => 1	10.5	1.6	10.7	1.6
		899 => 900	-0.1	17.4	-0.1	17.7

GCP ID	Video Product ID	Frame Number	dx (pixel)	dy (pixel)	dx (m)	dy (m)
P03	PDT2	0 => 1	-37.0	18.0	-33.7	16.4
		450 => 451	-12.2	29.9	-11.1	27.2
		899 => 900	-31.1	44.1	-28.3	40.1

Regarding the absolute accuracy, The RMSE values obtained in both directions are 22.6 m as shown in Table 3-3. The locations of the backprojected points are shown in Figures 7 and 8.

Table 3-3 Planimetric Accuracy Results of SkySat video frames (absolute, in meter unit).

Reference	GCP Set
Sample (#GCP)	5
Easting Error Mean (m)	-12.5 m
Northing Error Mean (m)	20.6 m
Easting Error STD (m)	16.7 m
Northing Error STD (m)	12.7 m
Easting Root Mean Square Error (m)	20.8 m
Northing Root Mean Square Error (m)	24.2 m
Root Mean Square Error (m)	22.6 m



Figure 3-7. GCP P20 image projected on the image
1307610184.98412180_sc00003_c1_PAN_i0000000000



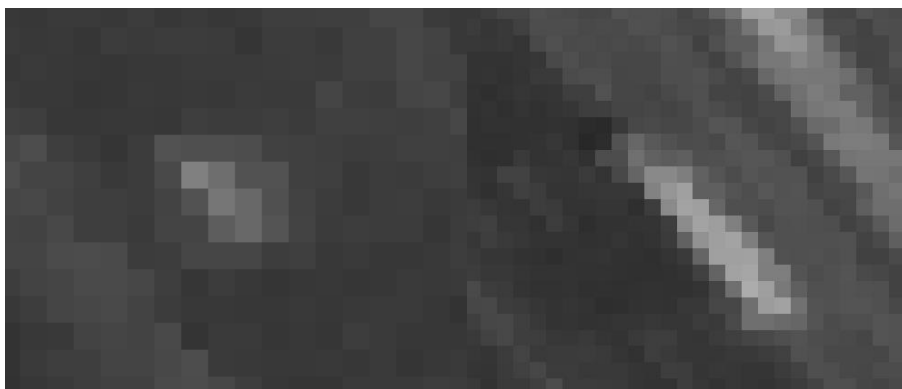
Figure 3-8. GCP P03 projected on the image
1308482688.04125881_sc00108_c1_PAN_i0000000000

3.4 Information Extraction Capability

In this section, the EDAP Team investigated the information extraction and motion analysis capability of video data. Although similar efforts with more details exist in the literature (e.g. see [RD-38, RD-42, RD-20, RD-22, RD-11, RD-24, RD-27, RD-25, RD-44, RD-31, RD-32, RD-28, RD-33, RD-35, RD-36, RD-40]), here the main goal was to investigate the quality metrics and point out potential issues in this field.

3.4.1 Methods and tools

Here, the main criteria for the method selection was the availability of open source libraries and the simplicity of the application. Considering the size and the radiometric properties of the vehicles, the template matching functionality of OpenCV in Python was used for object detection, [RD-21]. Templates of different vehicles are shown in Figure 3-9.



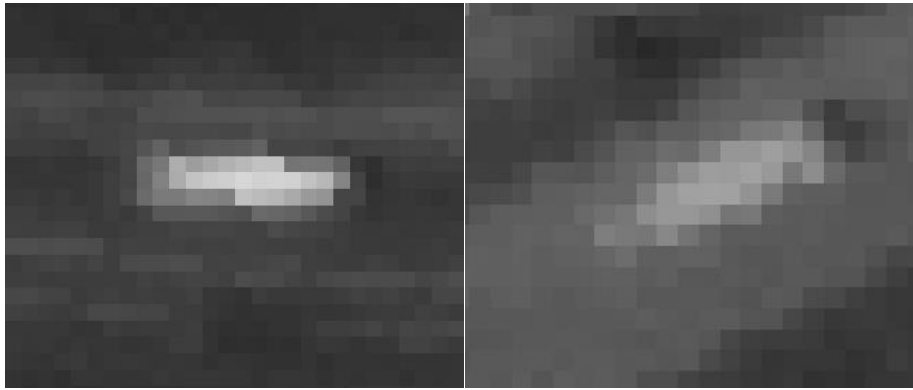


Figure 3-9. Template examples of vehicles used for detection and tracking.

Various OpenCV Object Tracker Implementations were investigated for object tracking [RD-21]. The investigated tracking methods include TrackerBoosting¹, CSRT², Kernelised Correlation Filter (KCF)³, medianFlow⁴, Multiple Instance Learning (MIL)⁵, Minimum Output Sum of Squared Error (MOSSE)⁶ and Tracking, learning and detection (TLD)⁷ [RD-22]. The algorithms were not specifically developed for satellite video, and therefore improvements can be expected with satellite specific methodology development.

3.4.2 Results

The evaluations within EDAP are only preliminary, and therefore the results for the different methods are not given separately. Instead, the different issues in processing are summarised. The literature examples for video data validation given in Section 2.6 (e.g. DEM generation, airplane or ship detection, river velocity analysis, etc.) are also not fully investigated here due to the data availability. Only vehicles such as cars, buses and trucks are detected and tracked within this information extraction capability context here.

In Figure 3-10 and Figure 3-11, examples as screenshots from the different stages of tracking are shown.

¹ Helmut Grabner, Michael Grabner, and Horst Bischof. *Real-time tracking via on-line boosting*. In *BMVC*, volume 1, page 6, 2006.

² Alan Lukežić, Tom'as Voj'ir, Luka Cehovin Zajc, Jir'i Matas, and Matej Kristan. *Discriminative correlation filter tracker with channel and spatial reliability*. *International Journal of Computer Vision*, 2018.

³ M. Danelljan, F.S. Khan, M. Felsberg, and J. van de Weijer. *Adaptive color attributes for real-time visual tracking*. In *Computer Vision and Pattern Recognition (CVPR)*, 2014 IEEE Conference on, pages 1090–1097, June 2014.

⁴ Zdenek Kalal, Krystian Mikolajczyk, and Jiri Matas. *Forward-backward error: Automatic detection of tracking failures*. In *Pattern Recognition (ICPR)*, 2010 20th International Conference on, pages 2756–2759. *IEEE*, 2010.

⁵ Boris Babenko, Ming-Hsuan Yang, and Serge Belongie. *Visual tracking with online multiple instance learning*. In *Computer Vision and Pattern Recognition, 2009. CVPR 2009. IEEE Conference on*, pages 983–990. *IEEE*, 2009.

⁶ David S. Bolme, J. Ross Beveridge, Bruce A. Draper, and Man Lui Yui. *Visual object tracking using adaptive correlation filters*. In *Conference on Computer Vision and Pattern Recognition (CVPR)*, 2010.

⁷ Zdenek Kalal, Krystian Mikolajczyk, and Jiri Matas. *Tracking-learning-detection*. *Pattern Analysis and Machine Intelligence*, *IEEE Transactions on*, 34(7):1409–1422, 2012.

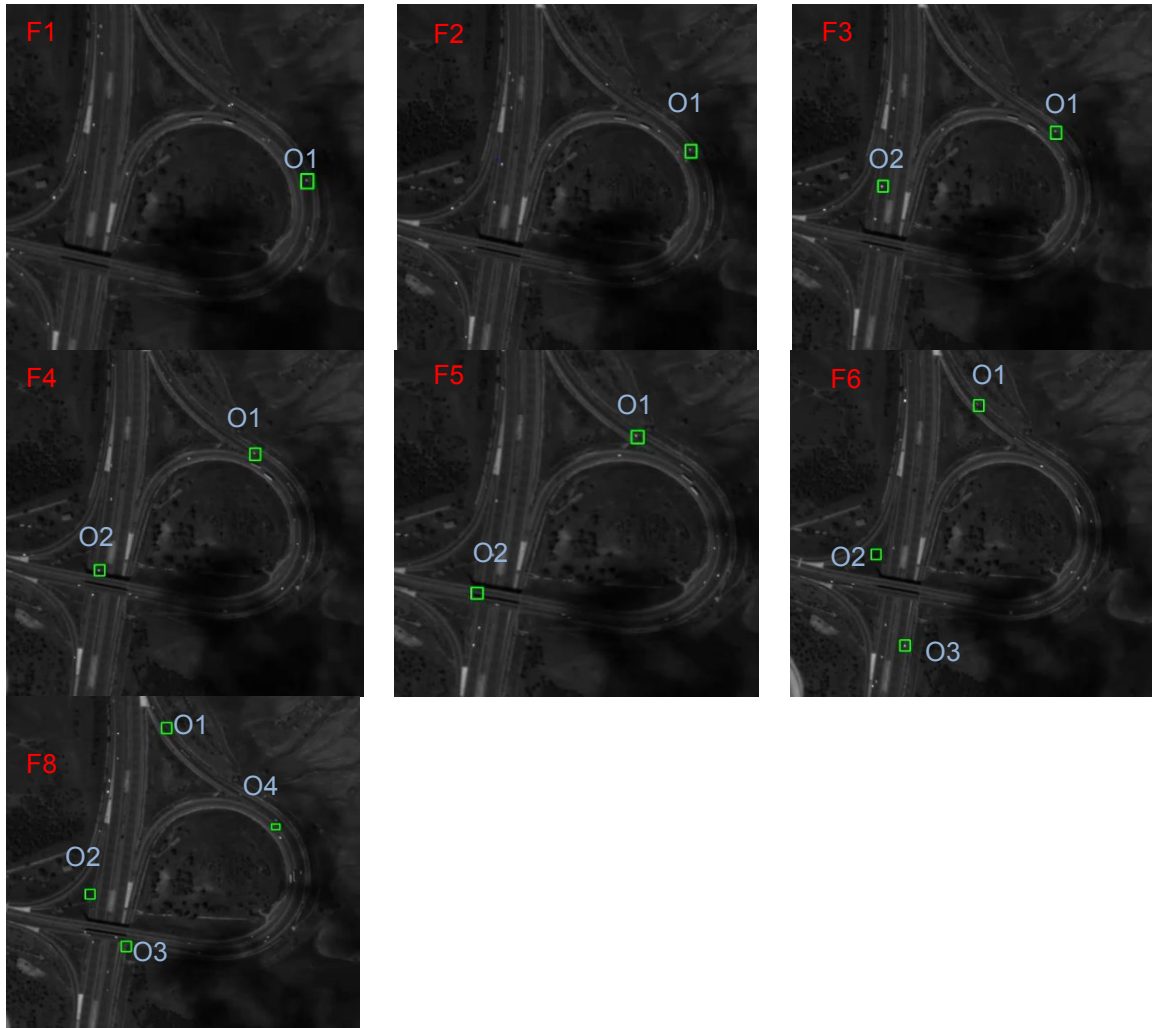


Figure 3-10. Multiple object tracking examples of vehicles in PDT2. Object 1 (O1) was lost in frame 6 (F6) due to another object coming from the opposite direction. O2 was lost in F4 due to the bridge. O3 was lost in F8 for the same reason. O4 entered the scene much later than the other objects.

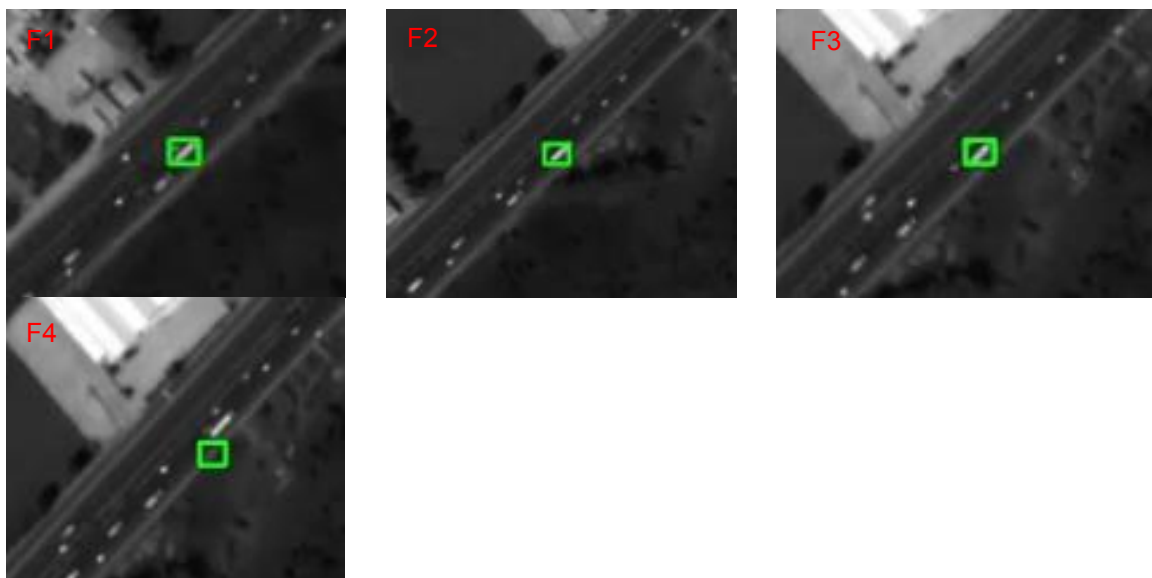


Figure 3-11. Single object tracking examples of vehicles in PDT2. Here, the tracked object was lost in F4 due to the other vehicles in the same lane.

The results have shown that multiple objects can be detected at the same time. The tracking is also possible, but the following problems due to algorithm / image quality were observed:

- The changes in object-background contrast causes the loss of the object. Objects having the same radiometric properties as the background are difficult to track.
- Although an object can be detected in the first frame and tracked until it is out of the frames, the detection stage needs to be repeated for the newly entering objects, which cause an increased amount of processing. Optimizations may be needed here.
- The objects in the same lane with different speeds cause losses or mis-tracking of the other objects. Objects in opposite lanes also suffer from the same problem.
- The tracking of the rotating objects is problematic in most algorithms since the shape and the orientation of the object changes in the image. A rotating template matching approach could be useful here.
- The size of the detectable and trackable objects are open to question. Although there are different criteria for the size of smallest objects detectable in an image, a 2x2 pixels object can be expected to be detected. The object-background contrast, image blurring and the other radiometric artefacts (e.g. striping) also play role here. Considering the GSD of the video data (ca. 1 m here), cars are expected to be detectable. Regarding the tracking, smaller sizes could be detectable with precise matching algorithms (e.g. least squares matching).
- Occlusions sources form by trees and high building cause interruptions or stop in the tracking.

APPENDIX A MISSION AND PRODUCT

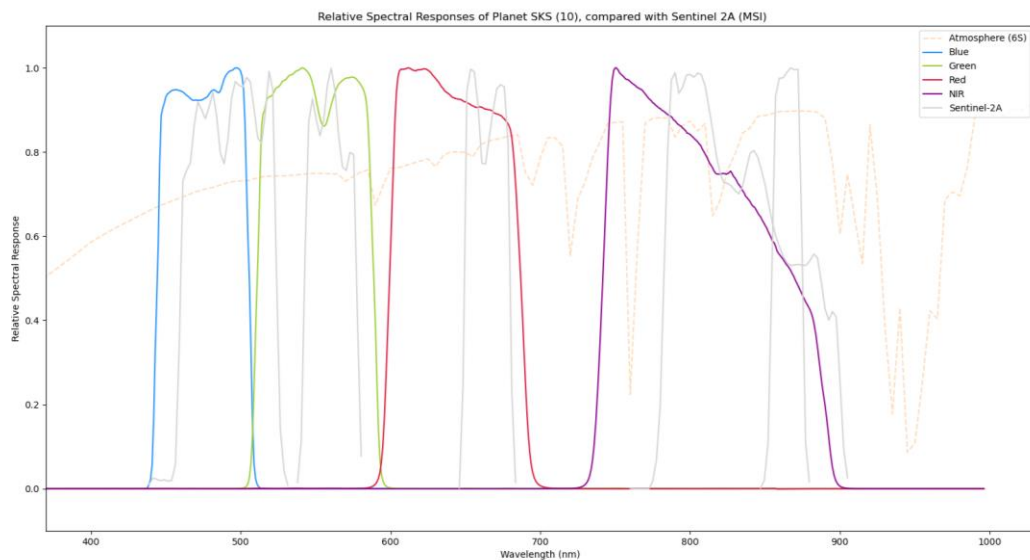
A.1 Mission Description

The SkySat constellation is the VHR component of Planets satellite image portfolio. Skysat-A and B generation satellites were launched in 2013/14. The SkySat-C generation satellite (60 x 60 x 95 cm) is a high-resolution Earth imaging satellite, first launched in 2016, all collecting thousands of square kilometres of imagery. Each satellite is 3-axis stabilised and agile enough to slew between different targets of interest. Furthermore, each satellite has four thrusters for orbital control, along with four reaction wheels and three magnetic torquers for attitude control. All SkySats contain Cassegrain telescopes with a focal length of 3.6m, with three 5.5 megapixel CMOS imaging detectors making up the focal plane.

Regarding the SkySat constellation, the full list of satellite is given in⁸ and report herein in Table 3-4: List of SkySat Satellites.

Imagery are captured in a continuous strip of single frame images known as "scenes", which are all acquired in the blue, green, red, NIR-infrared, and panchromatic bands, with following spectral bandwidth definition:

- Blue: 455 - 515 nm,
- Green: 500 - 590 nm,
- Red: 590 - 670 nm,
- NIR: 780 - 860 nm,
- Panchromatic band: 450-900 nm.



The RSR curves of SKS #10 are shown in

⁸ https://space.skyrocket.de/doc_sdat/skysat-3.htm (Visited in January 5, 2021)

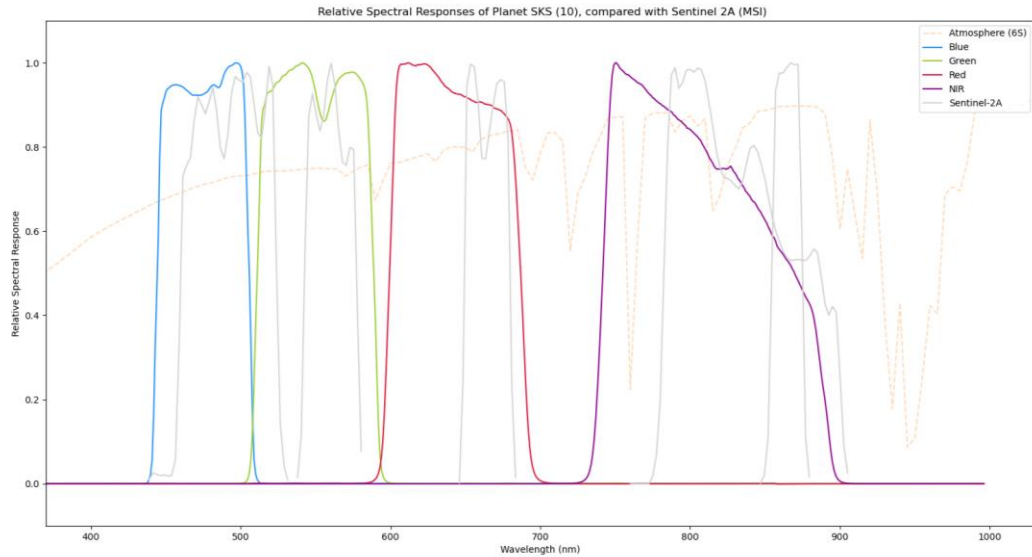


Figure 3-12 and compared with Sentinel-2 MSI ones. Furthermore, the atmospheric transmittance curve (obtained with 6S) is added in background. The spectral bandwidth of SKS RSRs is larger than Sentinel-2 ones. Moreover respective NIR central wavelength values (not shown in the figure) are shifted. Because both SKS, Sentinel-2 RSRs are of different shapes and localisation of H₂O absorption bands (NIR), the use of the proposed EDAP calibration approach is fully justified.

The ground sampling distance depends on the spectral channel and on the image mode. Latest products are observed with PBHDR is imaging mode. The PBHDR mode actually changes the capture settings of the spacecraft and the camera. It is not a processing method but an acquisition method. It is a way to artificially reduce the scan rate by vibrating the camera in synchronisation with the spacecraft velocity and frame rate. It allows to increase the SNR while also increasing the capacity of each spacecraft.

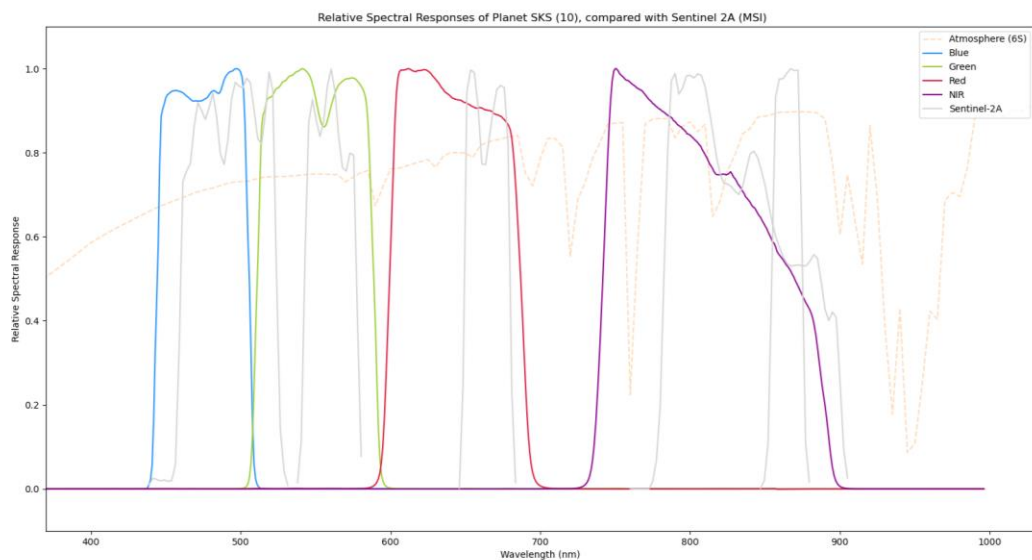


Figure 3-12: Comparison of SKS and Sentinel-2 RSRs together with atmospheric transmittance (6s) over a wavelength interval within 350 nm, 1000 nm interval.

Table 3-4: List of SkySat Satellites.

Satellite	COSPAR	Date	LS	Launch Vehicle	Remarks
SkySat 3 (SkySat C1)	2016-040C	22.06.2016	Sr SLP	PSLV-XL	with Cartosat 2C , BIROS , M3MSat , LAPAN A3 , GHGSat D , Flock-2p 1, ..., 12 , SathyabamaSat , Swayam , BeeSat 4
SkySat 4 (SkySat C2)	2016-058D	16.09.2016	Ko ELV	Vega	with PeruSat 1 , SkySat 5, SkySat 6, SkySat 7
SkySat 5 (SkySat C3)	2016-058E	16.09.2016	Ko ELV	Vega	with PeruSat 1 , SkySat 4, SkySat 6, SkySat 7
SkySat 6 (SkySat C4)	2016-058B	16.09.2016	Ko ELV	Vega	with PeruSat 1 , SkySat 4, SkySat 5, SkySat 7
SkySat 7 (SkySat C5)	2016-058C	16.09.2016	Ko ELV	Vega	with PeruSat 1 , SkySat 4, SkySat 5, SkySat 6
SkySat 8 (SkySat C6)	2017-068F	31.10.2017	Va 576E	Minotaur-C-XL-3210	with SkySat 9, SkySat 10, SkySat 11, SkySat 12, SkySat 13, Flock-3m 1, ..., 4
SkySat 9 (SkySat C7)	2017-068E	31.10.2017	Va 576E	Minotaur-C-XL-3210	with SkySat 8, SkySat 10, SkySat 11, SkySat 12, SkySat 13, Flock-3m 1, ..., 4
SkySat 10 (SkySat C8)	2017-068D	31.10.2017	Va 576E	Minotaur-C-XL-3210	with SkySat 8, SkySat 9, SkySat 11, SkySat 12, SkySat 13, Flock-3m 1, ..., 4
SkySat 11 (SkySat C9)	2017-068C	31.10.2017	Va 576E	Minotaur-C-XL-3210	with SkySat 8, SkySat 9, SkySat 10, SkySat 12, SkySat 13, Flock-3m 1, ..., 4
SkySat 12 (SkySat C10)	2017-068B	31.10.2017	Va 576E	Minotaur-C-XL-3210	with SkySat 8, SkySat 9, SkySat 10, SkySat 11, SkySat 13, Flock-3m 1, ..., 4
SkySat 13 (SkySat C11)	2017-068A	31.10.2017	Va 576E	Minotaur-C-XL-3210	with SkySat 8, SkySat 9, SkySat 10, SkySat 11, SkySat 12, Flock-3m 1, ..., 4
SkySat 14 (SkySat C12)	2018-099AR	03.12.2018	Va SLC-4E	Falcon-9 v1.2 (Block 5)	with SkySat 15, Eu:CROPIS , STPSat 5 , FalconSat 6 , NEXTSat 1 , KazSTSAT , eXCITE , SeeMe , ICEYE X2 , BlackSky Global 2 , ESEO , Hawk A, B, C , Capella 1 , AISTECHSAT 2 , CSIM-FD , Hiber 2 , ITASAT 1 , Landmapper-BC 4 , ORS 7A, 7B , Al-Farabi 2 , Astrocast 0.1 , Audacy 0 , BRIQ , Centauri 1 , Eaglet 1 , Enoch , Flock-3s 1, 2, 3 , K2SAT , KazSciSat 1 , MinXSS 2 , Orbital Reflector , RAAF M1 , SeaHawk 1 , SNUSAT 2 , THEA , VESTA , PW-Sat 2 , SNUGLITE , VisionCube , RANGE A, B , Elysium-Star 2 , ExseedSat 1 , Fox 1C , Irvine 02 , JY1-Sat , KNACKSAT , MOVE 2 , SpaceBEE 5, 6, 7 , Suomi-100 , WeissSat 1 , Sirion Pathfinder 2 , OrbWeaver 1, 2 , SPAWAR-CAL 0, OR, R
SkySat 15 (SkySat C13)	2018-099AW	03.12.2018	Va SLC-4E	Falcon-9 v1.2 (Block 5)	with SkySat 14, Eu:CROPIS , STPSat 5 , FalconSat 6 , NEXTSat 1 , KazSTSAT , eXCITE , SeeMe , ICEYE X2 , BlackSky Global 2 , ESEO , Hawk A, B, C , Capella 1 , AISTECHSAT 2 , CSIM-FD , Hiber 2 , ITASAT 1 , Landmapper-BC 4 , ORS 7A, 7B , Al-Farabi 2 , Astrocast 0.1 , Audacy 0 , BRIQ , Centauri 1 , Eaglet 1 , Enoch , Flock-3s 1, 2, 3 , K2SAT , KazSciSat 1 , MinXSS 2 , Orbital Reflector ,



					RAAF M1 , SeaHawk 1 , SNUSAT 2 , THEA , VESTA , PW-Sat 2 , SNUGLITE , VisionCube , RANGE A, B , Elysium-Star 2 , ExseedSat 1 , Fox 1C , Irvine 02 , JY1-Sat , KNACKSAT , MOVE 2 , SpaceBEE 5, 6, 7 , Suomi-100 , WeissSat 1 , Sirion Pathfinder 2 , OrbWeaver 1, 2 , SPAWAR-CAL O, OR, R
SkySat 16 (SkySat C14)	2020-038BL	13.06.2020	CC SLC-40	Falcon-9 v1.2 (Block 5)	with Starlink v1.0 8-1, ..., 8-58 , SkySat 17, SkySat 18
SkySat 17 (SkySat C15)	2020-038BM	13.06.2020	CC SLC-40	Falcon-9 v1.2 (Block 5)	with Starlink v1.0 8-1, ..., 8-58 , SkySat 16, SkySat 18
SkySat 18 (SkySat C16)	2020-038BN	13.06.2020	CC SLC-40	Falcon-9 v1.2 (Block 5)	with Starlink v1.0 8-1, ..., 8-58 , SkySat 16, SkySat 17
SkySat 19 (SkySat C17)	2020-057BQ	18.08.2020	CC SLC-40	Falcon-9 v1.2 (Block 5)	with Starlink v1.0 10-1, ..., 10-58 , SkySat 20, SkySat 21
SkySat 20 (SkySat C18)	2020-057BR	18.08.2020	CC SLC-40	Falcon-9 v1.2 (Block 5)	with Starlink v1.0 10-1, ..., 10-58 , SkySat 19, SkySat 21
SkySat 21 (SkySat C19)	2020-057BS	18.08.2020	CC SLC-40	Falcon-9 v1.2 (Block 5)	with Starlink v1.0 10-1, ..., 10-58 , SkySat 19, SkySat 20